JUNE 1980 PPPL-1669
UC-20f

CONF-800320--4

# FORBIDDEN LINES OF HIGHLY IONIZED IONS FOR LOCALIZED PLASMA DIAGNOSTICS

BY

E. HINNOV, R. FONCK, AND S. SUCKEWER



## PLASMA PHYSICS LABORATORY




PRINCETON UNIVERSITY
PRINCETON, NEW JERSEY

This work was supported by the U.S. Department of Energy Contract No. DE-AC02-76-CHO 3073. Reproduction, translation, publication, use and disposal, in whole or in part, by or for the United States government is permitted.

# Forbidden Lines of Highly Ionized Ions for Localized Plasma Diagnostics

E. Hinnov, R. Fonck and S. Suckewer

Princeton University, Plasma Physics Laboratory

Princeton, New Jersey 08544

Numerous optically forbidden lines resulting from magnetic dipole transitions in low-lying electron configurations of highly ionized Fe, Ti and Cr atoms have been identified in PLT and PDX tokamak discharges, and applied for localized diagnostics in the high-temperature (0.5-3.0 keV) interior of these plasmas. The measurements include determination of local ion densities and their variation in time, and of ion motions (ion temperature, plasma rotations) through Doppler effect of the lines. These forbidden lines are particularly appropriate for such measurements, because under typical tokamak conditions their emissivities are quite high ($10^{11}$ -$10^{14}$ photons/$cm^3$-sec), and their relatively long wavelengths allow the use of intricate optical techniques and instrumentation. The spatial location of the emissivity is directly measurable, and tends to occur near radii where the ionization potential of the ion in question is equal to the local electron temperature. In future larger and presumably higher-temperature tokamaks analogous measurements with somewhat heavier atoms, particularly krypton, and perhaps zirconium appear both feasible and desirable.

Presented at the Third APS Topical Conference on Plasma Diagnostics, Los Angeles, March 17-19, 1980

## 1. Introduction

In tokamak discharges during the quasi-steady phase, the radial temperature (and density) profiles are more-or less peaked [1-5], with usual peak values 1-2 keV in Ohmic heating, 3-4 keV with neutral-beam or other auxiliary heating. In future devices 5-10 keV peak temperatures may be expected.

For local diagnostics, e.g., measurements of ion temperature, plasma motions, localized oscillations or fluctuations, particle transport etc., it is essential to find some temperature dependent (hence radially localized) signals in the above mentioned temperature range. Radiation emitted by different ionization states by various medium-Z elements that commonly occur in tokamak plasmas (e.g., Ti, Cr, Fe, Ni, Mo) or may be added in small predetermined quantities for diagnostic purposes (e.g., Kr, Xe), provide such signals.

The radial range of a particular state of ionization of an element, with ionization potential $E_i$, is usually fairly limited [6,7] with the peak of the radial distribution generally in the neighborhood where the electron temperature is $T_e(r) \simeq E_i$. The deviations from coronal equilibrium, which predicts distribution peaks at lower temperatures, about $E_i \simeq 2\ T_e(r)$, are probably caused by radial ion transport rates, which may be sufficiently large to be competitive with ionization rates.

In the temperature range of primary interest in tokamaks, it is therefore the n = 2 or L-shell ions of the medium-Z elements that are particularly appropriate for diagnostics, because their ionization potentials are in the proper range. The strong resonance lines, corresponding to electric dipole transitions with $\Delta n = 0$ (i.e., $2s^2 2p^x - 2s2p^{x+1}$) of these ions lie in the wavelength range of about 70-200 Å. This is in the grazing-incidence region

of vacuum ultraviolet, a difficult region for high-resolution or absolute intensity measurements, with small solid angles available for light gathering, and practically no optics allowed. The $\Delta n \neq 0$ lines are in the 5-15 Å region, which is still worse.

Fortunately, in the $2s^2 2p^x$ (and the 2s2p) configurations there exist magnetic dipole transitions, and also some spin-forbidden intercombination lines, that may have sufficient intensity and more convenient wavelengths for diagnostic purposes. Several of these lines have been observed [7-9] and some have been applied to local diagnostics in the PLT and PDX tokamaks [5,10,11]. Figures 1 and 2 show the transitions and wavelengths of the observed lines in iron and titanium, respectively. Analogous sets of lines in other elements are shifted towards shorter wavelengths with increasing Z.

The wavelengths of these forbidden transitions are often approximately known from differences of measured wavelengths of allowed transitions [e.g., 12-16]. Some of the iron forbidden lines have been observed directly in solar flares [17]. Edlen [18] has devised semiempirical methods of describing the energy levels along isoelectronic sequences, and is currently preparing a comprehensive review that should allow adequate wavelength predictions up to at least nickel or copper. Tables of critically evaluated energy levels for several elements of tokamak interest have recently been published by the U.S. National Bureau of Standards [19].

At tokamak densities ($\sim 10^{14}/cm^3$) the rates of collisional excitation for the low-energy ($\Delta n = 0$) transitions under considerations are typically $10^4$-$10^5$/sec. The emissivity of the allowed resonance lines, with radiative transition rates $> 10^{10}$/sec, is therefore strictly determined by the collisional excitation rate; the emissivity varies linearly with the local electron density, and the corresponding excited state population is negligibly

small in comparison with ground-state population. The magnetic dipole radiative transition rates in the n = 2 ground configurations for $Z \gtrsim 22$ -28 are typically in the range $10^2$-$10^5$/sec (the magnetic dipole transitions scale roughly as $Z^{12}$ with the nuclear charge), i.e., comparable with the collisional transition rates. This relationship between excitation and radiative transition rates has several consequences, depending on the particular case: (1) the photon emissivity of the forbidden lines may be nearly comparable to the resonance lines, (2) the excited level populations may be a significant fraction of the total ion density, approaching Boltzmann equilibrium in cases of high electron density and low radiative rates, (3) the dominant excitation rate may be indirect, e.g., pumping through an excited configuration, $2s^22p^x - 2s2p^{x+1}$, and (4) the emissivity is in general not a linear function of electron density. For the last reason it is important to establish at least approximately the various potentially dominant collisional and radiative rates, in order to allow the use of the measured emissivity for ion density determination. Calculations of the emissivity-density relationship for a number of cases of tokamak or astrophysical interest have been made on the basis of approximate rate coefficients [7, 20, 21], and several recent calculations of radiative transition probabilities have been or are being published [22, 23, 24].

Because of the rapidly increasing radiative transition rate with atomic number, the n = 2 shell forbidden transitions beyond about nickel or copper will resemble allowed transitions at tokamak densities, i.e., their emissivities will be determined primarily by collisional excitation rate, and will be directly proportional to the electron density. In these heavier elements the analogous forbidden transitions in the n = 3 shell will also have radiative transition probabilities sufficiently large ( $\gtrsim 10^2$) to be of acute

interest in tokamak diagnostics.

## 2. Measurements in PLT Discharges

Figures 3-6 show samples of applications of the forbidden lines in diagnostics of various plasmas in the PLT tokamak. Ion temperatures during high-power neutral beam heating [5] in PLT were measured from Doppler broadening of the 2665 Å line of Fe XX and the 255 Å resonance line of Fe XXIV (Fig 3). Because of the usability of optics (mirrors and lenses) the former could be scanned repeatedly during a given discharge, and could thus follow the temporal temperature evolution throughout. The latter, scanned shot-by-shot with a grazing-incidence spectrometer, had too large uncertainties during the first 30-40 msec of injection partly caused by pulse-to-pulse irreproducibility and partly by the relatively small intensity of the line (as indicated by the lower graph) during this time. Fe XXIV is located somewhat closer to the center of the discharge, thus the measurements indicate an early centrally peaked $T_i(r)$ profile, which gradually broadens. The drop of $T_i$ while the beams were still on was caused by continued rise in plasma density.

Figure 4 shows ion temperature radial profile measurements, including Doppler profile measurements of the 2665 Å line of Fe XX and the 2117 Å line of Ti XIV [this line was erroneously reported [9] at 2115 Å ] during ion cyclotron resonance heating [25] in the PLT. (Both the temperatures and the power levels are considerably lower than in the neutral-beam case.) Typical results of toroidal plasma rotation measurements [10] during unidirectional neutral beam injection in PLT are shown in Fig. 5. The toroidal velocities were deduced from Doppler shifts of the lines, and the radial locations from spatial scans of their intensity distribution, measured by means of a system of rotating mirrors. A sample of such poloidal (minor-radius) scan, of the

Fe XX 2665 Å emissivity during and shortly after a neutral-beam injection in PLT is shown in Fig. 6, together with the emissivity of the CV 2271 Å line and some unidentified background radiation near the the 2665 Å wavelength. The background (and CV) radiation have quite different time-dependence from that of the Fe XX line, thus helping to discriminate the latter. The up-down asymmetry evident in the figure is quite typical in PLT discharges, being generally more pronounced nearer the periphery of the plasma. The graphite aperture limiter is located at ± 40 cm, and the CV light forms a quasicylindrical shell about 7 cm further inward. At larger radii, the electron temperature is too low for this line to be emitted, and at smaller radii, carbon is ionized further to CVI. Similarly, Fe XX forms a shell at around r = 10 cm after the neutral-beam injection (just before the beam, the emission was also quite similar to this), for analogous reasons. During the injection there was a substantial enhancement of the Fe XX radiation near the center. The details of this phenomenon are not yet well understood, although it appears probable that the lowering of iron ionization states through charge-exchange with beam-injected $H^0$ atoms had a significant role. The purpose of this figure is not to attempt to explain the evidently very complicated plasma dynamics, but to illustrate some typical features of the forbidden line emission and measurements: the radial location and extent, the frequent presence of potentially interferring radiation, and the often a priori unexpected behavior of the emissivity.

The phenomenon of charge-exchange recombination during high-power neutral-beam injection has been observed in more detail [26] by comparing the behavior of the lithium-like Fe XXIV and Ti XX and the boron-like Fe XXII densities in PLT discharges. In these measurements also the use of the forbidden line of Fe XXII was important - the large wavelength separation

allowed simultaneous scan of two ions with a two-channel grazing incidence spectrometer.

A particularly intriguing phenomenon currently under study in tokamak plasmas is the appearance of large-scale "sawtooth" oscillations that tend to appear often with unbalanced neutral-beam injection. They are radially localized, e.g., near-central Fe XXIV light may show almost 100% modulation, with a frequency of 20-30 msec (depending on injected power), whereas the simultaneously measured Fe XXII light, located slightly further outward, may be practically steady. (A qualitatively similar observation comparing Mo XXXI and Mo XXXII light has been reported in the TFR tokamak) [27]. At least part of the oscillations are due to temperature fluctuations as indicated by measurements of neutron emissivity [28], soft-x-ray continua [29] etc. As such fluctuations usually do not reproduce in detail from pulse to pulse, a large number simultaneous localized measurements is necessary to untangle the physical processes involved, and for this application the emission of the various ion forbidden lines appears particularly appropriate.

In all these cases mentioned in this Section, the measurements either became possible or were greatly facilitated by the relatively long wavelengths of the forbidden lines of the ions, and the interest in the measurements derives from the location of the ions, due to their large ionization potential, in the high-temperature part of the plasma.

## 3. Future Prospects

Figure 7 shows the wavelengths of the magnetic dipole lines of the $2s^2 2p^x$ configurations of several elements from titanium through krypton. The dotted lines are predicted but have not yet been definitely observed. In elements lighter than Ti, the transition probabilities become too small and in elements heavier than Kr the wavelengths become too short for convenient use. However,

as mentioned above, in heavier elements forbidden transitions in the n = 3 shell may be of interest, particularly in krypton and xenon, that can be readily admitted in controlled amounts to the discharge. Other heavy elements, such as zirconium, niobium or molybdenum may be used for special purposes in future tokamaks. The large total radiation efficiency of heavy atoms, of course, limits their admissibility to very small quantities ( $\lesssim 10^{10}/cm^3$), but this is sufficient for many applications.

A representative electron temperature (and density) radial profile in tokamak plasmas is shown in Fig. 8, together with approximate locations of these magnetic dipole lines (and also some convenient carbon and oxygen lines that have been frequently used in diagnostics), for central temperatures of 2 keV and 5 keV. The former is a typical value of present large tokamaks such as PLT or PDX, whereas the latter may be expected in large tokamaks in a few years. In the krypton spectrum, which does not attain the n = 2 shell at 2 keV in appreciable quantities, the $3p^3P_{3/2-1/2}$ line of the aluminum sequence is also indicated. Clearly, in this temperature range all these lines, and particularly those of the as yet unidentified lines of the heavier elements such as a nickel, copper and krypton are of major interest in spectroscopic diagnostics.

## Acknowledgments

All the measurements reported in this paper were possible only with the cooperaton and support of PLT and PDX tokamak operations and diagnostics groups.

This work has been supported by United States Department of Energy Contract No. DE-AC02-76-CHO-3073.

## References


[1] DIMOCK, D., EUBANK, H., HINNOV, E., JOHNSON, L. C, and MESERVEY, E., Nucl. Fusion 13 (1973) 271.

[2] EQUIPE TFR, Nucl. Fusion 15 (1979) 1053.

[3] HAWRYLUK, R., et al., Nucl. Fusion (1980) to be published.

[4] ISLER, R. L, and CRUME, E. L., Phys. Rev. Lett. 41, (1978) 1296.

[5] EUBANK, H., et al., Phys. Rev. Lett. 43, (1979) 270.

[6] HINNOV, E., Atomic and Molecular Processes in Controlled Thermonuclear Fusion Devicas, Proc. NATO Advanced Study Institue, 1979 M. R. C. McDOWELL and A. M. Ferendici, editors Plenum Press, New York, (1980).

[7] SUCKEWER, S., and HINNOV, E., Phys. Rev. A21 (1978) 578.

[8] SUCKEWER, S., AND HINNOV,E., Phys. Rev. Lett 41 (1979) 756.

[9] SUCKEWER, S., FONCK, R., and HINNOV, E., Phys. Rev. A21 (1980) 924.

[10] SUCKEWER, S., et al., Phys. Rev. Lett. 43 (1979), 207.

[11] SUCKEWER, S., et al., Nucl. Fusion 19 (1979) 1681.

[12] FAWCETT, B.C., Atomic Data and Nuclear Data Tables 16 (1975) 135.

[13] DOSCHEK, G. A. FELDMAN, U., COWAN, R. D., and COHEN, L., Astrop J. 188 (1974) 417.

[14] KONONOV, E. Ya., KOSHELEV, K. N., PODOBEDOVA, L. I., CHEKALIN, S. V., and CHURILOV, S. S., J. Phys., B 9 (1976) 565.

[15] BRETON, C., DE MICHELIS, C., FINKENTHAL, M., and MATTIOLI, M., Phys. Lett. A74 (1979) 57.

[16] LAWSON, K. D., and PEACOCK, N. J., Culham Laboratory Report CLM-P586, 1980 to be published.

[17] FELDMAN, U., DOSCHEK, G. A., COWAN, RD. D. AND COHEN, L., Astop. J. 196 (1975) 613.

[18] EDLEN, B., Solar Phyics 24, (1972) 356, Optica Pura y Aplicada 10

(1977) 123, and private communications, 1979, 1980.

[19] SUGAR, J., and CORLISS, C., J. Phys. and Chem. Reference Data 6 (1977) 317-383 (Cr), 6 1253-1329 (Mn), 8 (1979) 1-62 (Ti).

[20] MASON, H. E., DOSCHEK, G. A., FELDMAN, U., and BHATIA, A. K., Astron. Astrophys. 73 (1979) 74.

[21] FELDMAN, U., BHATIA, A. K., CHENG CHUNG-CHIEH, and DOSCHEK, G.A., J. Appl. Phys 51 (1980) 190.

[22] GLASS, R., J. Phys. B 13 (1980) 899.

[23] DANKWORT, W., and TREFFTZ., Astron. and Astrophysics 65, (1978), 93.

[24] MINA V-SAMII, DIN TON-THAT, and ARMSTRONG, L. (1980) (Johns Hopkins Univ. Report, to be published.)

[25] ROSEA, J., et al., Course and Workshop on Physics of Plasma Close to Thermonuclear Conditions, Varenna, Italy, 1979 Editrice Compositori, Bologna 1980.

[26] SUCKEWER, S., et al., Report PPPL-1636, Feb. 1980, to be published in Phys. Rev.

[27] BRETON, C., DE MICHELIS, C., FINKENTAHAL, M., and MATTIOLI, M., Phys. Rev. Lett. 41 (1978) 110.

[28] STRACHAN, J., et al., Report PPPL-TM-331 Feb. 1980, to be published.

[29] VON GOELER, S., et al., Phys. Rev. Lett. 33 (1974) 1201.

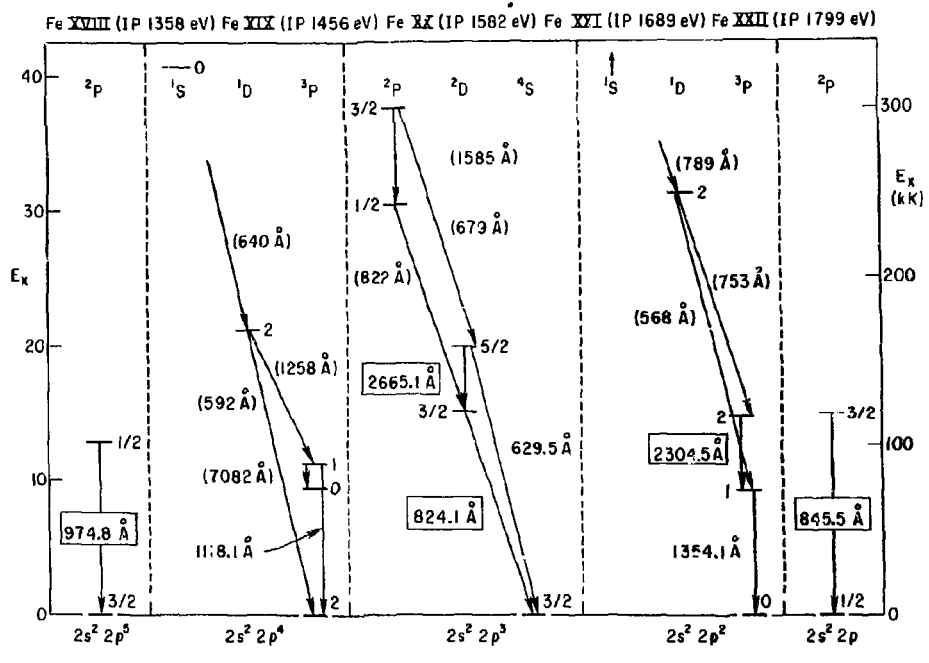


Fig. 1. Energy levels and wavelengths of forbidden transitions in $2s^2 2p^x$ configurations of iron. Wavelengths in boxes observed in PLT tokamak.

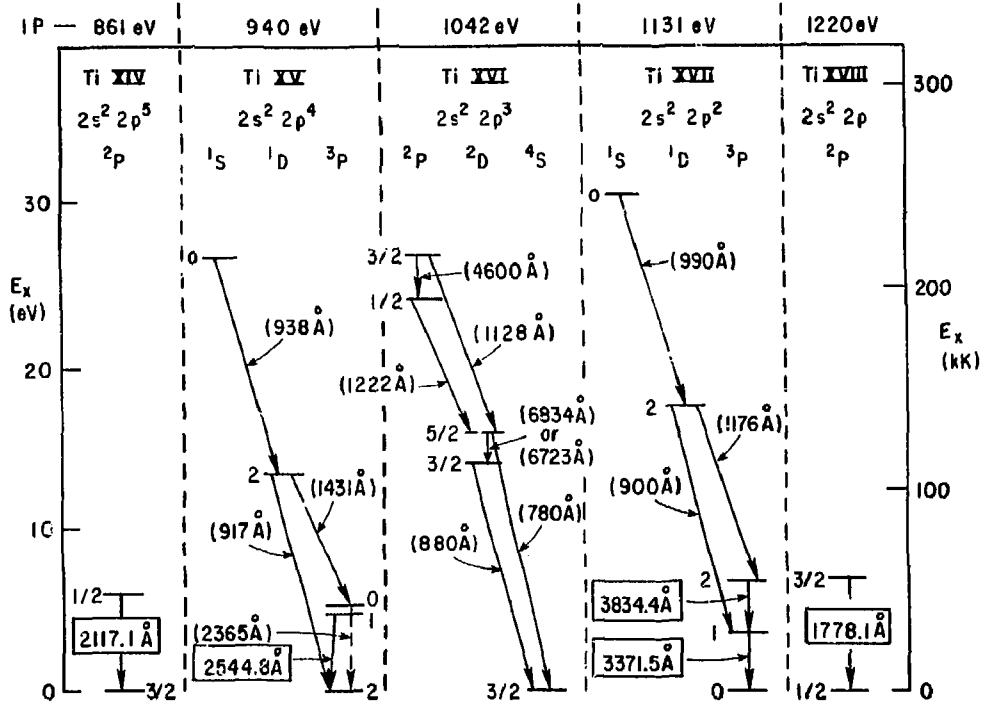


(PPPL-803651)

Fig. 2. Energy levels and wavelengths of forbidden transitions in $2s^2 2p^x$ configurations of titanium. Wavelengths in boxes observed in PDX and PLT.

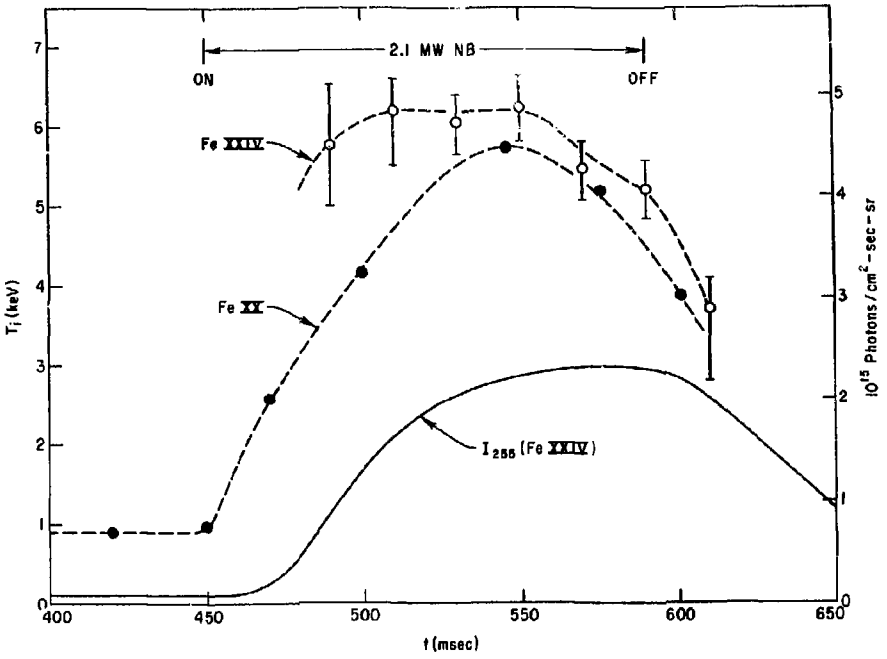


(PPPL-793847)

Fig. 1. Ion temperatures from Doppler broadening of Fe XX forbidden line at 2665 Å and Fe XXIV resonance line at 255 Å during neutral beam heating in PLT tokamak. The lower trace shows time evolution of the 255 Å line intensity.

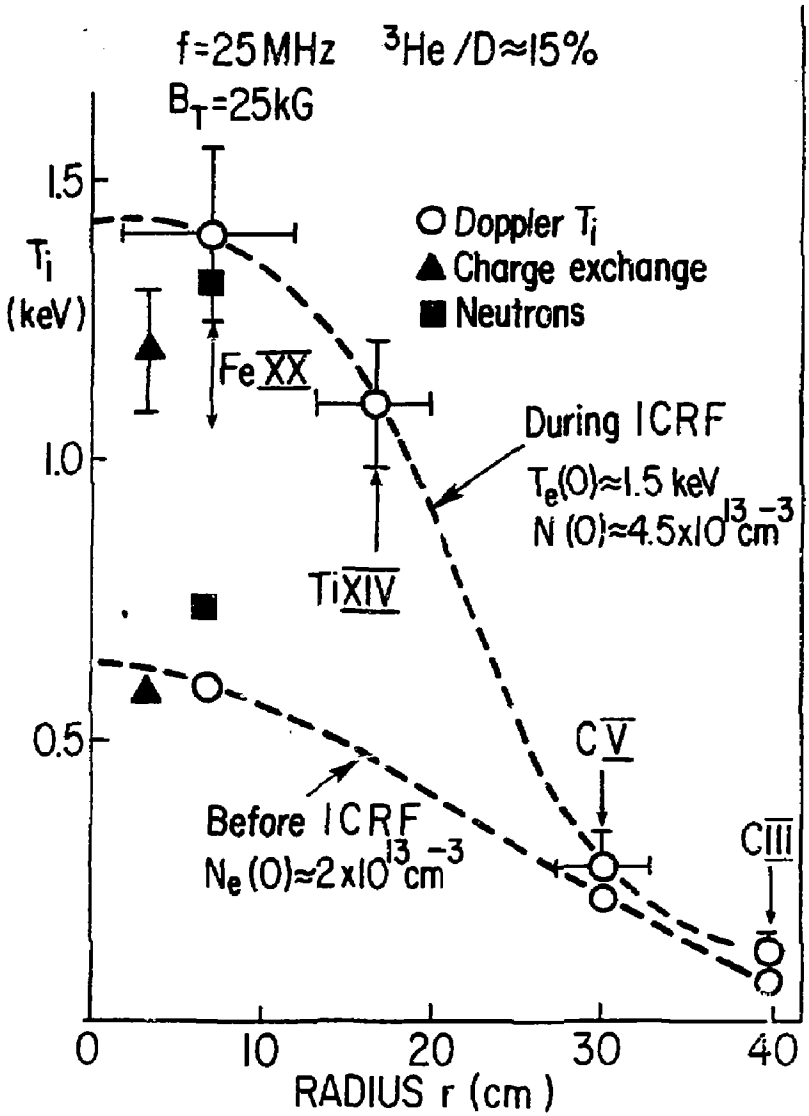


(PPPL-(4/30/80))

Fig. 4. Ion temperature profiles before and during ion cyclotron resonance heating in PLT.

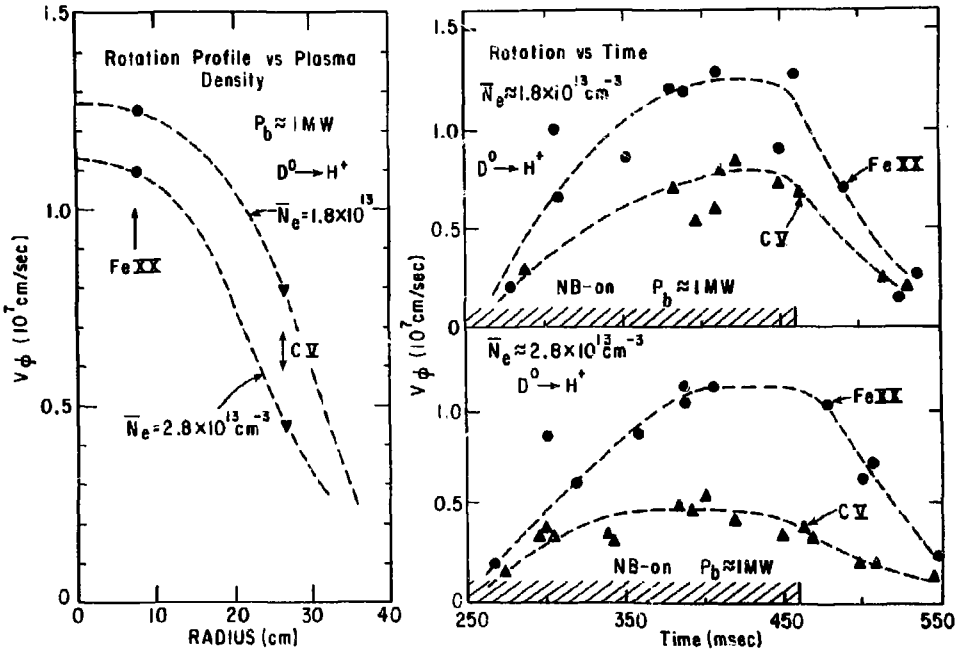


(PPPL-796385)

Fig. 5. Radial dependence and time evolution of toroidal rotation induced by unbalanced neutral beam injection in PLT, as deduced from Doppler shift and poloidal intensity measurements of Fe XX 2665 Å and CV 2271 Å lines.

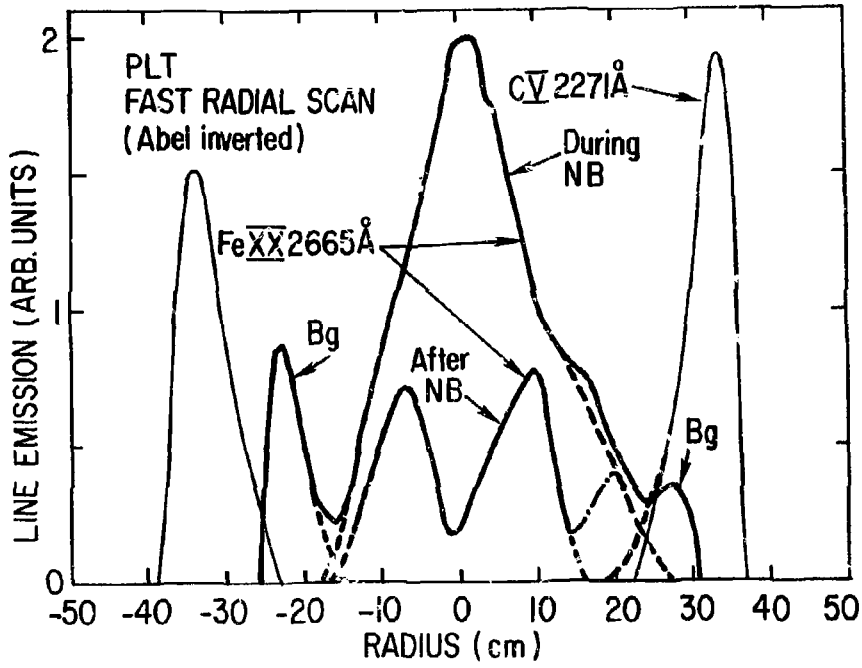


(PPPL-796569)

Fig. 6. Radial profiles of the 2665 Å line of Fe XX during and after a neutral beam injection in a moderate temperature PLT plasma. Profiles of CV and unidentified background radiation near 2665 Å were measured concurrently with the Fe XX line.

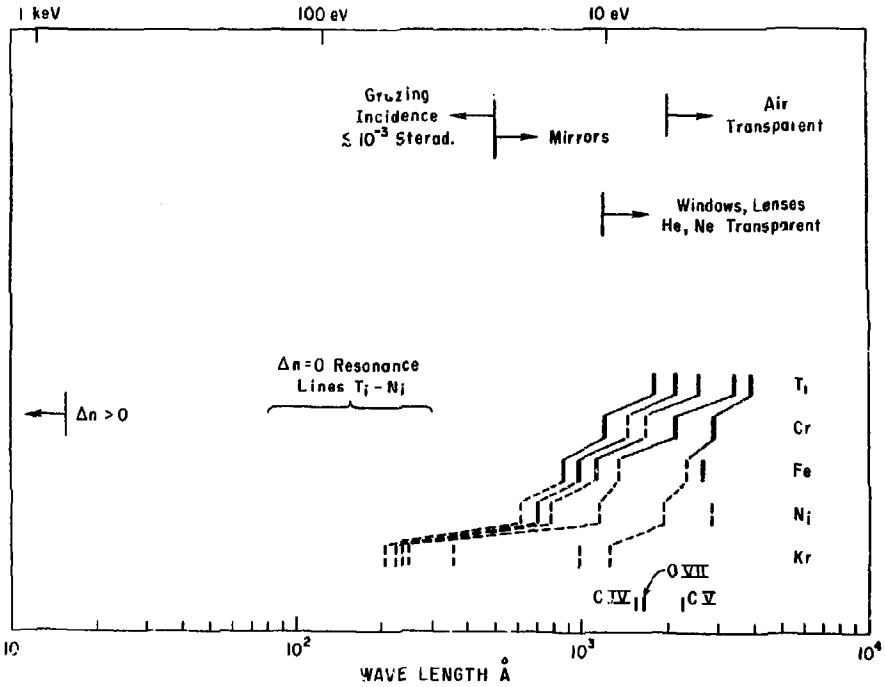


(PPPL-803641)

Fig. 7. Wavelength of measured and predicted (dotted lines) magnetic dipole lines in medium-Z elements of special interest in tokamak diagnostics.

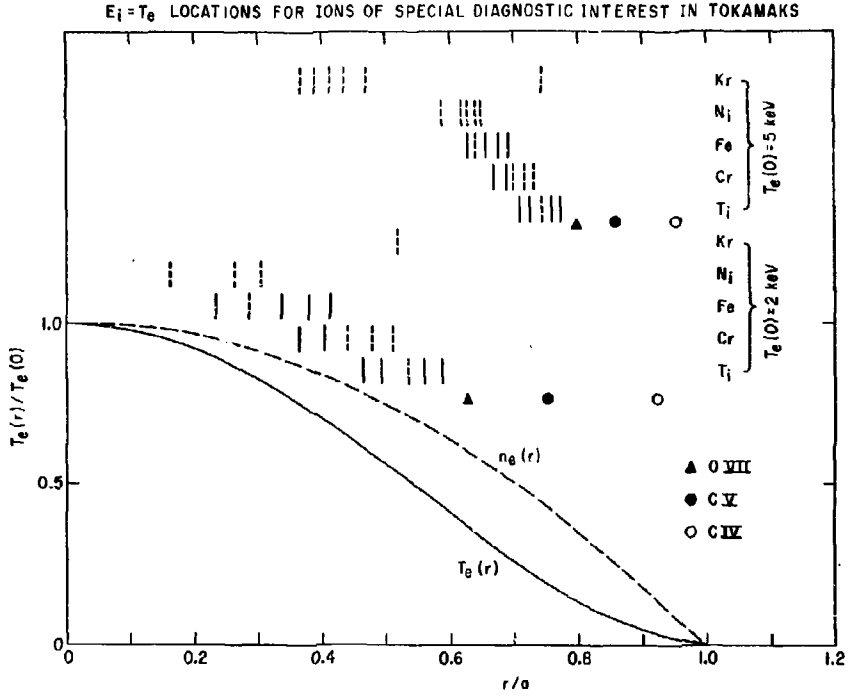


(PPPL-803334)

Fig. 8. Approximate positions of radiation maxima, assuming $E_i = T_e$, of the various magnetic dipole lines, and some popular carbon and oxygen lines in tokamak discharges with central temperatures 2 keV and 5 keV.